

## A new method for solving radiative heat problems in glass

***Citation for published version (APA):***

Linden, van der, B. J., & Mattheij, R. M. M. (2000). *A new method for solving radiative heat problems in glass*. (Corrected version ed.) (RANA : reports on applied and numerical analysis; Vol. 9906). Technische Universiteit Eindhoven.

***Document status and date:***

Published: 01/01/2000

***Document Version:***

Publisher's PDF, also known as Version of Record (includes final page, issue and volume numbers)

***Please check the document version of this publication:***

- A submitted manuscript is the version of the article upon submission and before peer-review. There can be important differences between the submitted version and the official published version of record. People interested in the research are advised to contact the author for the final version of the publication, or visit the DOI to the publisher's website.
- The final author version and the galley proof are versions of the publication after peer review.
- The final published version features the final layout of the paper including the volume, issue and page numbers.

[Link to publication](#)

***General rights***

Copyright and moral rights for the publications made accessible in the public portal are retained by the authors and/or other copyright owners and it is a condition of accessing publications that users recognise and abide by the legal requirements associated with these rights.

- Users may download and print one copy of any publication from the public portal for the purpose of private study or research.
- You may not further distribute the material or use it for any profit-making activity or commercial gain
- You may freely distribute the URL identifying the publication in the public portal.

If the publication is distributed under the terms of Article 25fa of the Dutch Copyright Act, indicated by the "Taverne" license above, please follow below link for the End User Agreement:

[www.tue.nl/taverne](http://www.tue.nl/taverne)

***Take down policy***

If you believe that this document breaches copyright please contact us at:

[openaccess@tue.nl](mailto:openaccess@tue.nl)

providing details and we will investigate your claim.

**RANA 99-06**  
**A new method for solving radiative heat  
problems in glass**

**B.J. van der Linden — R.M.M. Mattheij**  
**Scientific Computing Group**  
**Eindhoven University of Technology**  
**P.O.Box 513**  
**NL-5600 MB Eindhoven, The Netherlands**

**e-mail: [linden@win.tue.nl](mailto:linden@win.tue.nl)**

**15th May 2000**

### **Abstract**

In the production of glass, temperature plays a crucial role. However, until now, only crude approximations for radiative heat transfer have been used, although it represents the most influential mode of heat transfer. In this article the authors present two new methods that can help in the accurate calculation of radiative heat transfer. The first is a way to find directional sets of arbitrary size for the Discrete Ordinate Method. The second is an algebraic abstraction of the Ray Trace Method, which allows the use of this method without the need for re-tracing the geometry at every time or iteration step. Both methods are compared to existing methods.

# Contents

<b>1</b>	<b>Introduction</b>	<b>3</b>
<b>2</b>	<b>Radiative Heat Transfer</b>	<b>4</b>
2.1	Intensity and heat transfer . . . . .	4
2.2	Black body intensity . . . . .	5
2.3	Radiative transfer equation and heat transfer . . . . .	6
2.4	Gray medium . . . . .	6
<b>3</b>	<b>Discrete Ordinate Method</b>	<b>8</b>
3.1	Level Trapezium Method . . . . .	8
3.2	Homogeneous sets . . . . .	9
3.3	Comparison . . . . .	10
<b>4</b>	<b>Methods for one dimension</b>	<b>11</b>
4.1	Exact solution in one dimension . . . . .	11
4.1.1	Method of Solution . . . . .	13
4.1.2	Solution of the problem . . . . .	14
<b>5</b>	<b>Methods for calculating the intensity equations in higher dimensions</b>	<b>16</b>
5.1	Finite element solution . . . . .	16
5.2	Classical ray trace method . . . . .	17
5.2.1	Results . . . . .	19
5.3	Comparison and Conclusion . . . . .	20
<b>6</b>	<b>Methods for calculating heat transfer directly in more dimensions</b>	<b>21</b>
6.1	Algebraic form of the ray trace method . . . . .	21
6.2	Results . . . . .	23
<b>7</b>	<b>Conclusion</b>	<b>25</b>

# Chapter 1

## Introduction

The production of glass belongs to the oldest forms of human industrial production. After the discovery of glassy layers on pottery, man learned of the benefits of the use of glass. The material is strong though brittle; it can stand aggressive environments; and last but not least: it can be transparent. The manufacturing of glass happened on a small scale for a long time and glass products were used by a happy few. Industrialization led to mass production of glass. The methods of production, however, have hardly changed with the massification; usually manual operations are merely replaced by mechanical ones. Glass production in this way remains like wine making: although the necessary ingredients and proportions are known, the production is characterised by a process of trial-and-error on the shop floor. This process of trial-and-error is expensive, both economically and ecologically.

New environmental laws, the opening of the European market, and the growing competition from the plastic industries all have reduced the profit margin on glass mass products, making an optimization of the production cycle imperative. Most optimization has already been done through experience with trial-and-error techniques, but the limits of such optimization are almost reached. A call for deeper understanding of the mechanisms behind glass production is raised.

Two of the main research fields herein are chemistry and heat transfer. Glass results from a special mixture of ingredients producing a material that can easily be frozen in its liquid state. The reductor/oxidator condition of the glass melt strongly influences its temperature. And so are its physical properties during the forming process. A understanding of the temperature distribution in glass therefore stands at the base of understanding the processes.

## Chapter 2

# Radiative Heat Transfer

As mentioned before, one of the special features of glass is its transparency. It is this feature that causes the calculation of heat transfer to be more complicated than that in metals. Though both glass and metals are processed at elevated temperatures, the photons in metal can travel only small distances. This means that physically a particle only influences its direct neighbours and mathematically we end up with a differential equation: radiation in opaque materials behaves mathematically like conduction.

If we are dealing with a transparent material, the photons can travel through a large part of the domain in question. This means that in a mathematical sense we have to solve an integral equation: the temperature at a point is dependent on the temperature at any other point in the domain. Additional complications in glass production are the complex shapes that are involved. For example, if we look at the cooling of a hot bottle, we must realize that a particle within the bottom ‘sees’ through the bottom and through the empty part inside, the top of the bottle. We must be able to express this mathematically.

First, let us have a look at the equations describing radiative heat transfer. Radiation is the transfer of energy by photons. Thermal radiation limits itself to those photons that act on the temperature of particles in the medium. Typically these photons have associated wavelengths in the infrared domain of the electromagnetic spectrum. Here we hit the dual nature of electromagnetic radiation: it can be both described by particles and by waves. The former is used for derivation of stochastic methods like the Monte Carlo Method, where a great number of ‘photons’ is tracked. This method can lead to very accurate results, but the computational costs are high. The latter is the concept of radiation we use to derive our model. Note that macroscopically both views are identical.

### 2.1 Intensity and heat transfer

Starting from Maxwell’s electromagnetic wave equations, we can make some assumptions to end up with a simpler equation. If we consider unpolarised radiation (like Planckian radiation) in a dielectric medium (like glass), we can characterize radiation by a sole entity: the intensity.

The *monochromatic or spectral radiation intensity*  $I_\nu$  is defined as the amount of radiative energy travelling in a certain direction per unit area, per unit spherical angle, per unit frequency. Unlike heat flow, we cannot represent the intensity in a single vector, because photons and radiation will travel through a point in different directions. So, the intensity is a scalar depen-

dent on position and direction, or  $I_\nu = I_\nu(\mathbf{x}, \mathbf{s})$ . Here we already see the inherent complexity of radiation. Although we are dealing with a single scalar, it is dependent on six free variables: three spatial co-ordinates, two directional, and one for the frequency  $\nu$ .

Except for some measurement techniques like remote sensing or pyrometry, we generally are not interested in the intensity itself. We rather want to know the heat flux it generates. Looking at the definition of intensity, we see that for a particular wavelength/frequency the intensity represents the amount of energy per unit frequency per unit spherical angle travelling exactly in direction  $\mathbf{s}$ , or

$$\frac{\partial^2 \mathbf{q}_\nu^r}{\partial \nu \partial \Omega} = \mathbf{s} I_\nu.$$

If we integrate this over the entire unit sphere (which represents the space of directions) and over all frequencies, we find the radiative heat flux  $\mathbf{q}^r(\mathbf{x})$ :

$$\mathbf{q}^r(\mathbf{x}) = \int_{\nu=0}^{\infty} \int_{\Omega=4\pi} \mathbf{s} I_\nu d\Omega d\nu, \quad [2.1]$$

where  $4\pi$  means we should integrate over the entire unit sphere. So, if we know the intensity distribution, we also know the heat flux caused by the radiation.

## 2.2 Black body intensity

The entity that makes a direct link between temperature and intensity, is the black body intensity. A *black body* is a body that absorbs all incoming radiation without reflecting, scattering, or transmitting it. Now, we put such a body in an isothermal enclosure at temperature  $T$  and wait for thermal equilibrium to be reached. Because in thermal equilibrium the energy that enters a body equals that leaving the body, we find that a black body radiates with the maximum reachable intensity for temperature  $T$ . For an arbitrary frequency  $\nu$ , we call this the *spectral black body intensity*  $B_\nu$ . A black body emits radiation isotropically, so the black body is a function of position only:  $B_\nu = B_\nu(\mathbf{x})$ . Planck found (see [1], [7], and [5]) that the black-body intensity can be expressed in terms of the temperature of the enclosure (and therefore the temperature of the black body) as:

$$B_\nu(T) = \frac{2h\nu^3}{c^2 [e^{h\nu/kT} - 1]}, \quad [2.2]$$

where  $h$  is the Planck constant,  $k$  is the Boltzmann constant, and  $c$  is the speed of light in the medium. If we integrate this over all possible frequencies  $\nu$ , we find the *(total) black body intensity*  $B(T)$ :

$$B(T) = n^2 \frac{\bar{\sigma} T^4}{\pi}, \quad [2.3]$$

where  $n$  is the refractive index of the medium, and  $\bar{\sigma}$  is the Stefan-Boltzmann constant.

## 2.3 Radiative transfer equation and heat transfer

As radiation travels through the medium, the intensity along a ray changes due to absorption and emission within that medium. In general radiation is scattered, but if we look at glass melts far away from the batch mixture in the glass furnace, or at glass melts during the forming process, this scattering can be neglected.

If we look at the change of the intensity along a certain ray, which we write mathematically as  $\mathbf{s} \cdot \nabla I_\nu$ , we find a source due to emission by the hot medium and a sink due to absorption by the medium. The latter we express as follows. We introduce the *spectral absorption coefficient*  $\kappa_\nu$  which gives us the fraction of the intensity that gets absorbed per meter. So, the amount of intensity that is absorbed equals  $\kappa_\nu I_\nu$ . The derivation of the emission is somewhat more complicated. It is given by the Kirchhoff-Planck relation:

$$\eta_\nu = \kappa_\nu B_\nu, \quad [2.4]$$

where  $\eta_\nu$  stands for the emission at frequency  $\nu$ . This equation is actually valid only in *thermal equilibrium*, but we can use it with a high degree of accuracy if we have a *local thermal equilibrium* (LTE). For the assumption of LTE not to be valid, temperatures need to be even much higher than in a glass furnace, so we can use (2.4) for our application (see Chapter 6 of [5]). The *radiative transfer equation* then becomes:

$$\mathbf{s} \cdot \nabla I_\nu(\mathbf{x}, \mathbf{s}) = \kappa_\nu(\mathbf{x}) B_\nu(\mathbf{x}) - \kappa_\nu(\mathbf{x}) I_\nu(\mathbf{x}, \mathbf{s}). \quad [2.5]$$

If we assume furthermore diffusely reflecting boundaries, the boundary condition for (2.5) is

$$I_\nu(\mathbf{x}_w, \mathbf{s}) = \epsilon_\nu(\mathbf{x}_w) B_\nu(\mathbf{x}_w) + \frac{\rho_\nu(\mathbf{x}_w)}{\pi} \int_{\mathbf{n}(\mathbf{x}_w) \cdot \mathbf{s}' < 0} I_\nu(\mathbf{x}_w, \mathbf{s}') |\mathbf{n}(\mathbf{x}_w) \cdot \mathbf{s}'| d\Omega', \quad [2.6]$$

where  $\mathbf{n}(\mathbf{x}_w)$  is the normal at position  $\mathbf{x}_w$  on the boundary. Of course, this equation only prescribes the radiation leaving the boundary; in other words if  $\mathbf{n}(\mathbf{x}_w) \cdot \mathbf{s} > 0$ . The *spectral or monochromatic emissivity* of the wall is given by  $\epsilon_\nu$ ; the *spectral or monochromatic reflectivity* by  $\rho_\nu$ . If no radiation goes through the boundaries, as can be assumed in most applications for the glass industry, Kirchhoff's law requires that

$$\epsilon_\nu + \rho_\nu = 1.$$

## 2.4 Gray medium

To avoid complex notation for the derivation of subsequent methods, we will assume we are looking at a *gray medium*. For a gray medium the radiative properties are not dependent on the frequency, e.g.  $\kappa_\nu = \kappa$ . This is a violation of what happens in glass where we have typical lows and highs for certain frequencies (the water band, etc.), but the method can easily be upgraded to include various bands.

The radiative transfer equation for a gray medium can be expressed in the total rather than the spectral quantities:

$$\mathbf{s} \cdot \nabla I(\mathbf{x}, \mathbf{s}) = \kappa(\mathbf{x}) B(\mathbf{x}) - \kappa(\mathbf{x}) I(\mathbf{x}, \mathbf{s}). \quad [2.7]$$



with gray boundary conditions for diffusely reflecting boundaries given by

$$I(\mathbf{x}_w, \mathbf{s}_i) = \epsilon(\mathbf{x}_w)B(\mathbf{x}_w) + \frac{\rho(\mathbf{x}_w)}{\pi} \int_{\mathbf{n} \cdot \mathbf{s}' < 0} I(\mathbf{x}_w, \mathbf{s}') \mathbf{n} \cdot \mathbf{s}' d\Omega', \quad \forall \mathbf{s}_i \cdot \mathbf{n} > 0. \quad [2.8]$$

Similarly, the heat flux equation (2.1) can be written in these total quantities:

$$\mathbf{q}^r(\mathbf{x}) = \int_{4\pi} \mathbf{s} I(\mathbf{x}, \mathbf{s}) d\Omega. \quad [2.9]$$

## Chapter 3

# Discrete Ordinate Method

For a numerical approach we make use of the *Discrete Ordinate Method* (DOM). The idea behind the method is the following. Because it is numerically impossible to solve (2.7) for all possible — i.e. an infinite number of — directions, we choose a set  $\mathfrak{S}$  containing a finite number of directions we look at. Then, to be able to compute the integral in (2.9), we replace them by quadratures using the directions in  $\mathfrak{S}$  and corresponding weights  $w_i$ . In doing this, Equation (2.7) lets itself be rephrased as the system of equations

$$\mathbf{s}_i \cdot \nabla I(\mathbf{x}, \mathbf{s}_i) = \kappa(\mathbf{x})B(\mathbf{x}) - \kappa(\mathbf{x})I(\mathbf{x}, \mathbf{s}_i) \quad \forall \mathbf{s}_i \in \mathfrak{S},$$

with boundary conditions

$$I(\mathbf{x}_w, \mathbf{s}_i) = \epsilon(\mathbf{x}_w)B(\mathbf{x}_w) + \frac{\rho(\mathbf{x}_w)}{\pi} \sum_{\mathbf{n} \cdot \mathbf{s}_j < 0} w_j I(\mathbf{x}_w, \mathbf{s}_j) |\mathbf{n} \cdot \mathbf{s}_j|, \quad \forall \mathbf{s}_i \in \mathfrak{S}.$$

Now, we first concentrate on how to choose the set of directions  $\mathfrak{S}$ . Then we consider how to solve this system of equations, using two different methods: the *Finite Element Method* and the *Ray Tracing Method*.

The quality of the solution for using the DOM depends on the choice of directions and associated weights. Commonly, so-called *level symmetric sets* are used. These sets use the same set of direction cosines for each of the three axes. For an explanation and listing of these directions and associated weights, one can consult the report by Lathrop and Carlson [3].

### 3.1 Level Trapezium Method

Only a limited number of these sets have been tabulated. Therefore, we present here two different methods to obtain directions and weights, which both allow for a creation of an arbitrary number of directions. The first one is the *level trapezium method*. Basically we are looking for a quadrature that integrates accurately over a sphere, or

$$\int_{4\pi} f(\mathbf{s})d\Omega = \int_0^\pi d\vartheta \sin \vartheta \int_0^{2\pi} d\varphi f(\vartheta, \varphi) = \sum_{i,j} w_{ij} f(\mathbf{s}_{ij}).$$

To do this we choose the directions along certain levels  $\vartheta = \vartheta_i$ , ( $i = 1, \dots, N_L$ ). Then, on every level, we choose the trapezoidal rule to integrate over  $\varphi$  as this method gives super-convergence for periodic integrands. The number of directions on level  $i$  should depend on

its radius,  $\sin \vartheta_i$ . Like in level symmetric sets, we put  $1 \times 4$  directions on level  $\vartheta_1$ ,  $2 \times 4$  directions on level  $\vartheta_2$ , etc. We choose the values for  $\vartheta_i$  such that the number of directions on a level match the number of levels:

$$\vartheta_i = \arcsin \frac{i}{N_L}, \quad i = 1, 2, \dots, N_L,$$

$$\varphi_{ij} = \frac{\pi}{2} \frac{2j+1}{2i}, \quad j = 1, 2, \dots, i.$$

The weights  $w_{ij}$  belonging to the direction determined by  $(\vartheta_i, \varphi_{ij})$  can be calculated from

$$w_{ij} = w_i^\vartheta w_{ij}^\varphi.$$

Here,  $w_{ij}^\varphi$  is the weight found for the trapezoidal rule with  $4i$  directions on a level,

$$w_{i,j}^\varphi = \frac{\pi}{2i},$$

The weight  $w_i^\vartheta$  is given by

$$w_i^\vartheta = \int_{\arcsin a_i}^{\arcsin b_i} \sin \vartheta d\vartheta = \cos \arcsin a_i - \cos \arcsin b_i = \sqrt{1 - a_i^2} - \sqrt{1 - b_i^2},$$

where

$$\begin{aligned} a_i &= \frac{2i - 1}{2N_L}, & i &= 2, 3, \dots, N_L, & a_1 &= 0 \\ b_i &= \frac{2i + 1}{2N_L}, & i &= 1, 2, \dots, N_L - 1, & b_{N_L} &= 1. \end{aligned}$$

### 3.2 Homogeneous sets

Based on intuition, we would like to have direction sets where all directions have equal weights. Furthermore, if we associate every direction with a point on the unit sphere, we would like the distances between any direction ‘point’ and its neighbours all to be equal, such that the distribution of directions is completely symmetric. Unfortunately, this is only possible for the five possible regular solids, namely the tetrahedron, cube, octahedron, dodecahedron and icosahedron, with 4, 8, 6, 20 and 12 points (or directions) respectively. All of these regular solids have too few points to be of real interest.

So it is not possible to find direction sets with an arbitrary number of directions with equal distances between neighbours, but we can try to get as close to this ideal distribution as possible. Therefore we started experimenting with direction sets which can best be associated with electrons divided on the unit sphere. Due to the magnetic forces, these electrons would take positions such that their potential energy is minimized. The difference between this direction set and our ‘ideal’ direction set is that the *average* distance between one point and *all* the others is equal for every point, instead of the distances between one point and its direct neighbours.

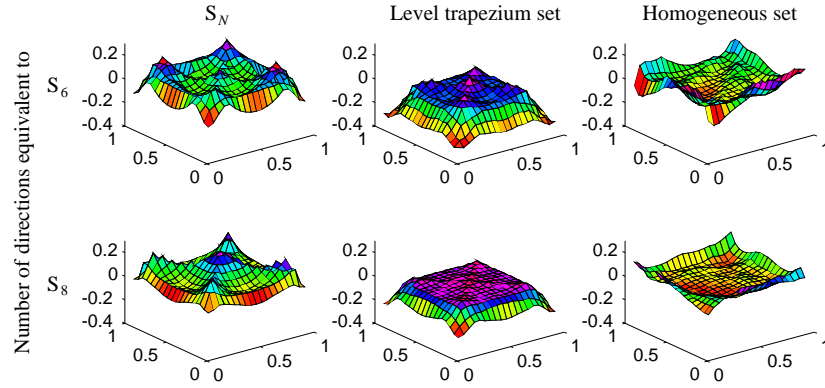


Figure 3.1: Error of the incident radiation as calculated by the discrete ordinates method using the  $S_N$ -, the level trapezium and the homogeneous direction sets.

### 3.3 Comparison

Consider the two-dimensional model problem of an absorbing-emitting medium inside a unit square surrounded by cold black walls ( $B(\mathbf{x}) = 1$ ). Using the discrete ordinates method with the  $S_N$ -, level trapezoidal and homogeneous direction sets the incident radiation — the intensity in a certain point integrated over all directions — inside the square has been calculated. In Figure 3.1, we see a plot of the difference between the discrete ordinates solution and the exact solution.

First of all we note that the level trapezium and homogeneous direction sets compare well with the  $S_N$  direction sets. It appears that the level trapezium method is more accurate than the  $S_N$  method on the interior domain, whereas at the boundaries the  $S_N$  method yields better results. An exception is the  $S_8$  direction set that gives results inferior not only to the level trapezium method with 80 directions but also to the  $S_6$  method. So the convergence of the  $S_N$  method for an increasing number of directions is not so reliable as the level trapezium method which seems to converge nicely.

Compared to the level trapezium method the homogeneous sets result in good approximations on the interior as well as on the boundary. The  $S_N$  sets are still superior on the boundary of the domain, but overall the homogeneous sets are more accurate than the  $S_N$  sets. Another advantage of the homogeneous sets is that they are reliable. We see no excessive values in any of the points and the method converges nicely for an increasing number of directions.

The largest errors of all methods occur at the boundary of the domain. This can be explained by the fact that near the boundary of the domain the derivatives of  $I(\mathbf{x}, \vartheta, \varphi)$  to  $\varphi$  and  $\vartheta$  are largest, causing the quadrature scheme to be less accurate. Especially near the corner points this effect occurs more dramatically, as can be seen in the plots of Figure 3.1.

## Chapter 4

# Methods for one dimension

The classical method to treat radiative heat problems — the so-called Rosseland or diffusion approximation — bypasses the complexity of the intensity calculations by solving the radiative transfer equations formally, and apply the formal solution to obtain an expression for the radiative heat transfer in terms of the black body intensity. Then, the assumption of optical thickness of the problem is made, which simplifies the expressions significantly. It can be shown that in the one-dimensional case, the assumption of optical thickness is equivalent to following a discrete ordinate method using only two directions. For a detailed discussion of this approximation we may refer to [6] and [7]. Here we only state the result for a gray medium without scattering, as we use this expression later in this paper:

$$\mathbf{q}^r = -\frac{4\pi}{3\kappa} \nabla B(\mathbf{x}). \quad [4.1]$$

This equation also carries the name *diffusion approximation*. Indeed, after applying the definition for  $B$  (2.3), (4.1) can be put into the following form:

$$\mathbf{q}^r = -k^r \nabla T,$$

which is similar to the expression for the conductive heat flow, also called the diffusive term in heat calculations. Because the radiative ‘conductivity’  $k^r$  is proportional to  $T^3$  the radiative diffusion term is highly non-linear, compared to the conductivity term. The expression can be applied in a straightforward manner, however. The major drawback of this method is the inaccuracy where the assumption of optical thickness is violated: close to the boundaries and for steep temperature gradients. This makes the method unfit to study the behaviour of the heat transfer at the walls of a glass furnace, or the re-heating process in the production of bottles.

In this section, we use a method to eliminate the intensity from the equations without making the severe constraint of optical thickness. We start by studying the (simple) one-dimensional equations and extend the results to higher dimensions.

### 4.1 Exact solution in one dimension

If scattering is neglected, the radiative transfer equation (2.7) can be simplified for the quasi-one-dimensional case into the following equations. Here, we mean with quasi-one-dimensional

that we do not restrict the directions to one dimension. Doing so would result in Rosseland-like solutions.

$$\tilde{\mu} \frac{\partial I^+}{\partial \tau}(\tau, \tilde{\mu}) + I^+(\tau, \tilde{\mu}) = B(\tau), \quad [4.2]$$

$$-\tilde{\mu} \frac{\partial I^-}{\partial \tau}(\tau, \tilde{\mu}) + I^-(\tau, \tilde{\mu}) = B(\tau), \quad [4.3]$$

where  $I^+$  and  $I^-$  are the intensities with directions that have components in positive and negative  $x$ -direction respectively. Furthermore,  $\tau = \int_x \kappa(x) dx$  is the dimensionless optical co-ordinate, and  $\tilde{\mu} = |\cos \vartheta|$ , where  $\vartheta$  is the angle of the direction vector with the  $x$ -axis. We wrote the intensity in two different components  $I^+$  and  $I^-$  with a  $\tilde{\mu} \in (0, 1]$ , because it simplifies relations that follow.

If we look at the problem on the open interval  $x \in (x_0, x_1)$ , with the corresponding dimensionless optical co-ordinate  $\tau \in (0, \tau_1)$ , the formal solution for the above equations is:

$$I^+(\tau, \tilde{\mu}) = c_0 e^{-\tau/\tilde{\mu}} + \frac{1}{\tilde{\mu}} \int_0^\tau e^{(s-\tau)/\tilde{\mu}} B(s) ds; \quad [4.4]$$

$$I^-(\tau, \tilde{\mu}) = c_1 e^{-\tau/\tilde{\mu}} + \frac{1}{\tilde{\mu}} \int_\tau^{\tau_1} e^{(\tau-s)/\tilde{\mu}} B(s) ds. \quad [4.5]$$

In the case of black boundaries, the two constants become  $c_0 = B_0 = B(0)$  and  $c_1 = B_1 = B(\tau_1)$ . This solution is only formal, since it is exactly the black body radiation  $B(\tau)$ , which—directly linked to the temperature—we are trying to find. This formal solution allows us, however, to find an expression for the radiative heat flux defined as:

$$q^r(\tau) = \int_{-\pi}^\pi d\phi \int_0^1 (I^+ - I^-) d\tilde{\mu} \tilde{\mu} = 2\pi \int_0^1 \tilde{\mu} (I^+ - I^-) d\tilde{\mu}. \quad [4.6]$$

Upon substituting (4.4) and (4.5) into (4.6) and assuming black boundaries, this can be elaborated to give:

$$\begin{aligned} q^r(\tau) = & 2\pi B_0 E_3(\tau) + 2\pi \int_0^\tau E_2(\tau - s) B(s) ds - \\ & 2\pi B_1 E_3(\tau) - 2\pi \int_\tau^{\tau_1} E_2(s - \tau) B(s) ds \end{aligned}$$

with  $E_n$  being the exponential integral of the  $n^{\text{th}}$  order, which are special functions that are explained in detail in Appendix A of [7]. We can use this equation as the radiative term in heat transfer equations. The simplest of these we arguably find by neglecting the other modes of heat transfer. In the one-dimensional case, this equation simply becomes:

$$\frac{dq^r}{d\tau}(\tau) = 0.$$

In this case, consequently, the black body radiation has to satisfy

$$B(\tau) = \frac{1}{2} \int_0^{\tau_1} E_1(|s - \tau|) B(s) ds + \frac{B_0}{2} E_2(\tau) + \frac{B_1}{2} E_2(\tau_1 - \tau). \quad [4.7]$$

### 4.1.1 Method of Solution

To solve the integral equation (4.7) we rephrase the problem in an abstract form:

$$x(t) = \int_0^a K(|s-t|)x(s)ds + g(t),$$

where  $x(t)$  is the function to be found,  $K(|s-t|)$  is the so-called *kernel* of the integral equation, and  $g(t)$  is the source function. This notation is chosen so both the pure one-dimensional (where  $K(|s-t|) = \exp(-|s-t|)$ ) as the quasi-one-dimensional case (where  $K(|s-t|) = E_1(|s-t|)$ ) can be treated by the same algorithm.

Using a projection method, we estimate the solution  $x(t)$  by

$$x(t) = \sum_i x(t_i)\phi_i(t).$$

This assumption transforms the integral equation (4.1.1) into

$$\sum_i x(t_i)\phi_i(t) = \sum_j x(t_j) \int_0^a K(|s-t|)\phi_j(s)ds + g(t).$$

Now, we use simplex functions for the base functions of the approximation:

$$\phi_i = \begin{cases} \frac{t-t_{i-1}}{t_i-t_{i-1}}, & t_{i-1} < t \leq t_i \\ \frac{t-t_{i+1}}{t_i-t_{i+1}}, & t_i < t < t_{i+1} \\ 0, & \text{elsewhere} \end{cases},$$

which have the nice property that

$$\phi_i(t_j) = \delta_{ij},$$

If we evolve the integral at points  $t_j$ , the integral equation becomes

$$x(t_i) = \sum_j x(t_j) \int_{t_{j-1}}^{t_{j+1}} K(|s-t_i|)\phi_j(s)ds + g(t_i).$$

We now introduce  $\psi_{ij}$  defined as:

$$\psi_{ij} = \int_{t_{j-1}}^{t_{j+1}} K(|s-t_i|)\phi_j(s)ds.$$

So, we can write the equation as:

$$x_i = \sum \psi_{ij}x_j + g_i, \quad \text{or} \quad \mathbf{x} = \Psi\mathbf{x} + \mathbf{g}.$$

Hence, the approximate solution can be found by solving

$$(I - \Psi)\mathbf{x} = \mathbf{g}. \tag{4.8}$$

The computational problem here now lies primarily in the  $N^2$  integral evaluations needed to compute  $\Psi$ . It can be shown, however, that when an equidistant grid is chosen, only  $N$  evaluations are needed and when stored in a certain vector  $\mathbf{f}$ ,  $\Psi$  satisfies

$$\psi_{ij} = f_{1+|i-j|}. \tag{4.9}$$

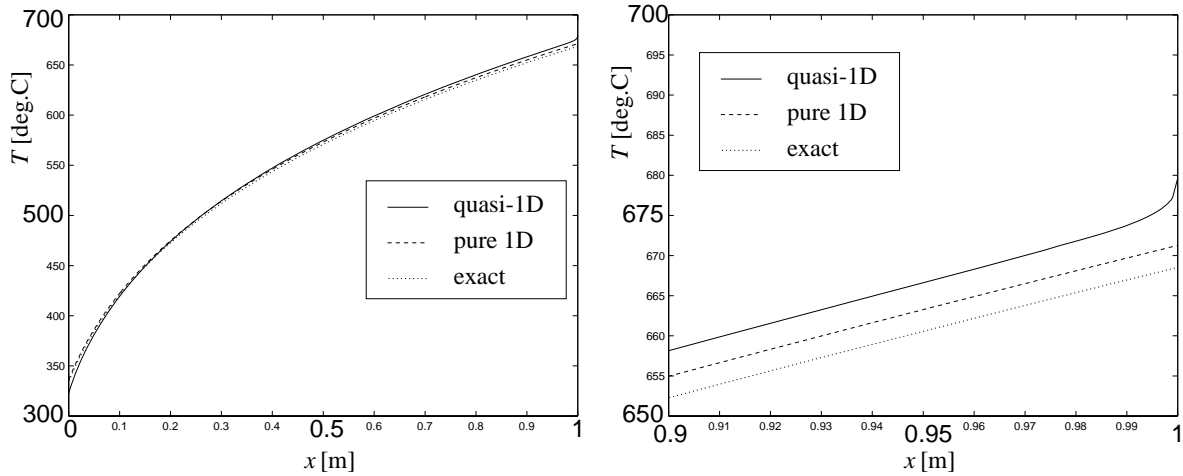


Figure 4.1: Temperature distribution in a thick glass rod (left) with detail close to the boundary (right)

### 4.1.2 Solution of the problem

Here, we present the results obtained by the above method. The  $\Psi$ -matrix has been constructed using a C++ implementation, whereas the linear problem (4.8) has been solved straightforwardly. Figure 4.1 shows the temperature distribution in a 1 m long glass rod. The material properties used for this are those of green bottle glass. Scattering has been neglected. From this figure we see that the quasi-one-dimensional case follows that of the purely one dimensional case (i.e. a Rosseland approximation) closely, except for the edges where the temperature jump is reduced.

If we consider thin geometries, the difference between the quasi and purely one-dimensional cases becomes more apparent as the effects near the edges spread over the whole domain of the problem (see Figure 4.2). The numerically computed results for the purely one-dimensional case now precisely match the analytically found solution, not having the offset as in the thick geometry. This numerical accuracy is due to a better conditioned matrix. The condition number of the matrix is approximately equal to 1 in the optically thin case, whereas we have a condition number of 150 in the optically thick case.



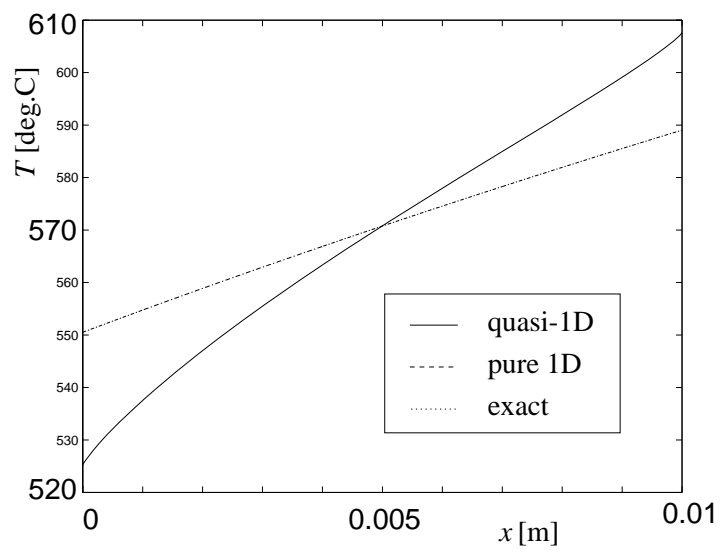


Figure 4.2: Temperature distribution in a thin rod (1cm)

## Chapter 5

# Methods for calculating the intensity equations in higher dimensions

Numerical solutions are usually sought in solving the radiative transfer equation (2.7) first. These methods use this as a step before the calculation of the radiative heat flux as given by (2.9). In this section we present two of those methods. The first uses the Finite Element Method (FEM), a method which is also used frequently for the two other modes of heat transfer: conduction and convection. Thus, for the whole heat transfer computation, the same method can be used. The second method is ray tracing. Here we actively follow the rays. It presents a versatile method that is better fit for specular reflecting boundaries and can deal with phenomena like refraction at transitions between media. It is in these situations that the FEM cannot be used any longer.

### 5.1 Finite element solution

In many practical problems, radiation appears together with conduction and/or convection. For these modes of heat transfer usually a finite element approach is used to compute the solution. Therefore, it seems attractive to derive a finite element method for the radiative transfer to combine the total energy transport into one general solution method.

A straightforward FEM formulation of (2.7), leads to problems as it is not unconditionally stable. Results will therefore not be reliable in cases of steep temperature gradients or irregular boundaries. One way to overcome this was presented by Fiveland [2]. This method uses the *even-parity* equations. Rather than calculating the intensity itself, we split it in the directionally even and uneven  $\varphi$  and  $\psi$ , which are defined by

$$\begin{aligned}\varphi(\mathbf{x}, \mathbf{s}) &= \frac{1}{2} [I(\mathbf{x}, \mathbf{s}) + I(\mathbf{x}, -\mathbf{s})], \\ \psi(\mathbf{x}, \mathbf{s}) &= \frac{1}{2} [I(\mathbf{x}, \mathbf{s}) - I(\mathbf{x}, -\mathbf{s})].\end{aligned}$$

Using (2.7) for uniform scattering — i.e. the Hopf phase function is taken  $\Psi(\mathbf{x}, \mathbf{s}', \mathbf{s}) = 1$  — with constant absorption and scattering coefficients, we can deduce the following relations

for these functions:

$$\varphi_\tau(\mathbf{x}, \mathbf{s}) + \psi(\mathbf{x}, \mathbf{s}) = (1 - \omega)B(\mathbf{x}) + \frac{\omega}{4\pi} \int_{4\pi} \psi(\mathbf{x}, \mathbf{s}', \mathbf{s}) I(\mathbf{x}, \mathbf{s}') d\Omega', \quad [5.1]$$

$$\psi_\tau(\mathbf{x}, \mathbf{s}) + \varphi(\mathbf{x}, \mathbf{s}) = 0, \quad [5.2]$$

with corresponding boundary conditions

$$\psi(\mathbf{x}_w, \mathbf{s}) + \varphi(\mathbf{x}_w, \mathbf{s}) = \epsilon B(\mathbf{x}_w) + (1 - \epsilon) \frac{q(\mathbf{x}_w)}{\pi}, \quad \mathbf{s} \cdot \mathbf{n} > 0, \quad [5.3]$$

$$\psi(\mathbf{x}_w, \mathbf{s}) - \varphi(\mathbf{x}_w, \mathbf{s}) = \epsilon B(\mathbf{x}_w) + (1 - \epsilon) \frac{q(\mathbf{x}_w)}{\pi}, \quad \mathbf{s} \cdot \mathbf{n} < 0. \quad [5.4]$$

Here,  $(\bullet)_\tau$  stands for differentiation with respect to  $\tau$ , defined as the dimensionless optical length defined by  $d\tau = \beta d\zeta$ , and where  $\zeta$  is the physical length along a ray. Finally,  $q(\mathbf{x}_w)$  is the energy incident on the wall from (2.8):  $q(\mathbf{x}_w) = \int_{\cap} I(\mathbf{x}_w, \mathbf{s}') |\mathbf{n} \cdot \mathbf{s}'| d\Omega'$ .

From these equations  $\varphi$  can be eliminated and we find the following expression governing  $\psi$ :

$$-\psi_{\tau\tau}(\mathbf{x}, \mathbf{s}) + \psi(\mathbf{x}, \mathbf{s}) = S(\mathbf{x}, \mathbf{s}), \quad [5.5]$$

where  $S(\mathbf{x}, \mathbf{s})$  is the source term which is equal to the right hand side in (5.1). We note that the equation for  $\psi$  is elliptic rather than hyperbolic as was (2.7). If scattering is present — i.e.  $\omega > 0$  — the source term is dependent on the solution. A way to by-pass this is the use of global iterations, so the second term in the source function can stay on the right hand side. Now let  $\Lambda$  be the domain of interest,  $\Gamma$  its boundary, and  $w \in \mathfrak{W}$  an arbitrary element in the space of all test functions on  $\Lambda$ . Then the weak formulation of (5.5) with boundary conditions (5.3) and (5.4) is given by:

$$\int_{\Gamma} w\psi |\mathbf{n} \cdot \mathbf{s}'| d\Gamma + \int_{\Lambda} w_s \psi_s + w\psi d\Lambda = \int_{\Lambda} wS(\mathbf{x}, \mathbf{s}) d\Lambda - \int_{\Gamma} w \left( \epsilon B(\mathbf{x}) + \frac{1 - \epsilon}{\pi} q(\mathbf{x}) \right) |\mathbf{n} \cdot \mathbf{s}'| d\Gamma$$

This equation can now be solved for discrete directions using the discrete ordinate method. Figure 5.1 shows the errors made by the DOM and the FEM for the case of constant  $B$ . Furthermore, the medium is assumed to be gray and  $\kappa$  to be constant. From this figure we see that enlarging the number of elements has almost no influence on the solution. Improvement should be made in the direction set before using more elements.

## 5.2 Classical ray trace method

Ray tracing is as the words indicate: it traces rays, using the radiative transfer equation (2.7) to calculate the change in intensity along the ray. Here we examine ray tracing in a two-dimensional space: both the geometry and the set of directions are chosen to be in  $\mathbb{R}^2$ . In the two dimensional space consider the domain  $\Omega$ . The boundary  $\Gamma$  is diffusely reflecting. On the geometry  $(\Omega, \Gamma)$ , we define a mesh consisting of (two-dimensional) surface and (one-dimensional) boundary elements. Our goal is to compute the total incident radiative energy for every element in the mesh.

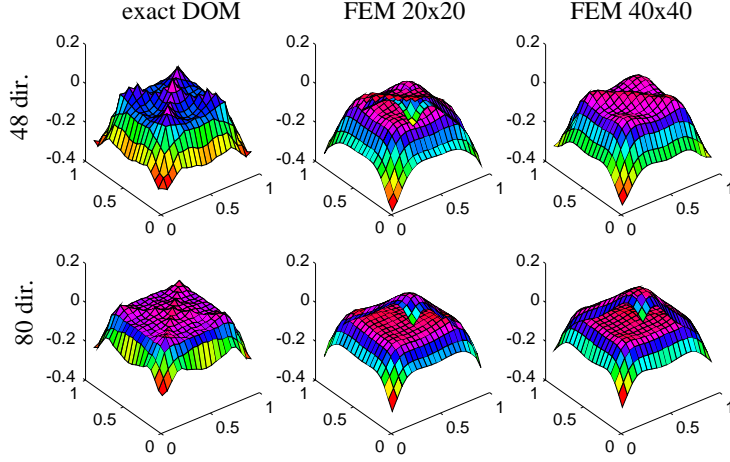


Figure 5.1: Total error of the DOM solved exactly and using a FEM with  $20 \times 20$  and  $40 \times 40$  elements respectively.

Before the calculation starts, every element  $e$  has a certain amount of emissive energy  $E_e$  depending on its temperature  $T_e$  and on its size. For simplicity, we assume here that the medium and boundary are gray and diffuse, but the extension to general media is almost trivial. The total amount of emissive energy in an element can be written as:

$$\begin{aligned} E_e &= \sigma A_e T_e^4, & (\text{surface element}), \\ E_w &= \sigma L_w T_w^4, & (\text{boundary element}), \end{aligned}$$

where  $A_e$  is the area of surface element  $e$  and  $L_w$  denotes the length of the boundary line element  $w$ . In every element the emissive radiation is initiated using the given directional discretization  $(s_i, w_i)$ . The initial intensity of a ray with direction  $s_i$  in a surface element is

$$I = \frac{1}{\pi} E_e = \frac{\sigma A_e}{\pi} T_e^4,$$

and the initial intensity of a ray which starts at the boundary is

$$I = \frac{1}{\pi} E_w (s_i \cdot \mathbf{n}).$$

Here,  $E_w$  is the sum of emissive and reflective energy stored in the boundary element and  $s_i$  is such that  $s_i \cdot \mathbf{n} > 0$ . We note that in the case of a scattering medium and a diffusely reflecting boundary every ray initiates many new rays, which in turn initiates even more. During the computation the number of rays would therefore become unbounded. To solve this problem, we do not initiate those new rays directly, but act as if the medium were non-scattering and the boundary were black. The difference is that in every element the total amount of *scattering energy* is raised each time a ray crosses that element. In the same fashion, we also introduce the total *reflective energy* for every boundary element. When all emitted rays have been absorbed, these scattered and reflected energies are used to initiate new rays. The solution is therefore found iteratively.

Every time a ray crosses a certain element, some energy of the ray is absorbed and the total incident energy of the element is raised. Since the incident energy is defined as an integral

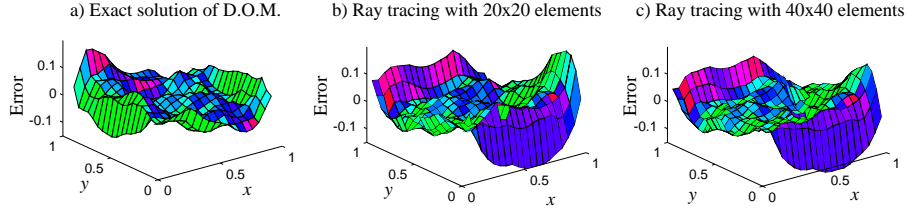


Figure 5.2: Error of the ray tracing method using the homogeneous direction set with 12 (2D) directions and  $20 \times 20$  resp.  $40 \times 40$  elements.

over the direction, we make use of the given direction discretisation using  $N_{\text{dir}}$  directions, i.e.

$$G_e = (1 - \omega) \int_{4\pi} I(\mathbf{s}) d\Omega = (1 - \omega) \sum_{i=1}^{N_{\text{dir}}} w_i I(\mathbf{s}_i).$$

Also the total amount of scattering energy  $E_e^s$  and reflection energy  $E_e^r$  can be written as an integral over

$$E_e^s = \omega \int_{4\pi} I(\mathbf{s}) d\Omega = \omega \sum_{i=1}^{N_{\text{dir}}} w_i I(\mathbf{s}_i),$$

$$E_e^r = \frac{\rho}{\pi} \int_{\mathbf{s} \cdot \mathbf{n} > 0} I(\mathbf{s}) |\mathbf{s} \cdot \mathbf{n}| d\Omega = \frac{\rho}{\pi} \sum_{i=1}^{N_{\text{dir}}} w_i I(\mathbf{s}_i) |\mathbf{s}_i \cdot \mathbf{n}|.$$

So, suppose a ray with intensity  $I$  and direction  $\mathbf{s}_i$  enters surface element  $e$ . This ray travels through the element for a (optical) distance  $\ell$ . Then due to absorption and scattering the change in intensity  $I$ , incident energy  $G_e$  and scattering energy  $E_e^s$  is

$$G_e = G_e + w_i(1 - \omega)Ie^{-\ell}$$

$$E_e^s = E_e^s + w_i\omega Ie^{-\ell}$$

$$I = Ie^{-\ell}$$

The case of a ray which hits a boundary element  $w$  leads to the following operations:

$$E_e^r = E_e^r + \frac{\rho}{\pi} w_i I |\mathbf{s}_i \cdot \mathbf{n}|$$

$$I = 0$$

### 5.2.1 Results

In Figure 5.2 we see the results as calculated by the ray tracing method using a homogeneous direction set with 12 directions. It turns out that the errors as given by the ray tracing method are of the same order of magnitude as the errors of the exact solution of the discrete ordinates method. This is not at all surprising, since the directions are used to approximate the same integrals as in the discrete ordinates method.

When we compare the errors of the solution on the  $20 \times 20$  mesh with the one on the  $40 \times 40$  mesh, we see that the errors do not change significantly. In fact, the difference between the two solutions is smaller than 0.04 everywhere on the domain, which is only one tenth of the total error.

### 5.3 Comparison and Conclusion

Comparing Figures 5.1 and 5.2, we see that for both methods the order of magnitude of the error is the same. Furthermore, if we denote the number of elements by  $N_{\text{el}}$  and—like before—the number of directions by  $N_{\text{dir}}$ , one can show that the computational cost of the ray trace method is

$$\text{Ray tracing : } O(N_{\text{dir}}N_{\text{el}}^{3/2}),$$

whereas the FEM would take a time-complexity of

$$\text{FEM : } O(N_{\text{dir}}(3N_{\text{el}})^p), \quad \frac{5}{4} \leq p \leq \frac{3}{2}.$$

Here  $p$  is dependent on the type of solver and preconditioner used.

So we see, that also with respect to time-complexity, the two methods are quite equivalent, but both have their own field of application: The FEM in combination with slug flows where a FEM is usually already used to solve such a flow problem; the ray trace method on the other hand for complex domains or non-smooth boundary conditions.

Furthermore, it is clear that a good direction set with appropriate weights is essential for the DOM to work. For that purpose, we have presented in Section 3 a method to find a good quadrature for arbitrary many directions.

## Chapter 6

# Methods for calculating heat transfer directly in more dimensions

Looking at the previous methods, it seems a waste to compute the intensity, largely being an entity we are not interested in. Only in some cases we care about knowing the intensity. An example might be remote sensing to determine the temperature profile by examining the radiation coming out of an object. But even then, we only want to know the intensity in some parts of the geometry and in only a few directions. So, is there a way to by-pass the intensity equations?

In Section 4.1 we derived such a method using the formal solution of the Radiative Transfer Equation. The Rosseland approximation is derived in a similar way. Here we decide to express the formal solution in more dimensions by using an algebraic form of the Ray Trace Method. This allows all flexibility—handling of reflections and refractions being the most important features—of this method to be present in our method. For an adapted Rosseland approximation that takes care of the geometry see [4].

### 6.1 Algebraic form of the ray trace method

Suppose, we want to know the temperature in a certain domain at  $M$  positions in the set of points  $\mathfrak{M} = \{\mathbf{x}_j, j = 1, 2, \dots, M\}$ . Rather than at an infinite number of directions, we only look at  $N$  discrete directions from the set  $\mathfrak{S} = \{\mathbf{s}_i | \mathbf{s}_i \in \mathbb{R}^3 \wedge \|\mathbf{s}_i\| = 1, i = 1, 2, \dots, N\}$ .

If we want to know the intensity at the  $j$ -th point (i.e. the point with co-ordinates  $\mathbf{x}_j$ ) in the  $i$ -th direction (direction is  $\mathbf{s}_i$ ), we trace the ray from that point back to the boundary. On the line we construct, say  $P^{ij}$  points and interpolate at those points the value of the black body intensity using only the points in  $\mathfrak{M}$ . If we place the black body intensity at the  $M$  points in a vector  $\mathbf{b}$  defined as:

$$\mathbf{b} = (B(\mathbf{x}_1), B(\mathbf{x}_2), \dots, B(\mathbf{x}_M))^T, \quad [6.1]$$

we can write black body intensity on the  $P^{ij}$  points on the ray as a vector  $\mathbf{p}^{ij}$  described by:

$$\mathbf{p}^{ij} = \mathbf{T}^{ij} \mathbf{b}, \quad [6.2]$$

in which  $\mathbf{T}^{ij}$  is an  $M \times P^{ij}$  matrix describing the interpolation coefficients at position  $j$  in direction  $i$ . For simple interpolations, involving only a small subset (typically with two or

three elements),  $\mathbf{T}^{ij}$  is sparse. Furthermore,  $\mathbf{T}^{ij}$  is determined geometrically and needs to be determined only once.

For simplicity, we now assume that scattering is absent within the medium, so the inhomogeneous part of the radiative transfer equations is formed by the black body intensity only. Then the ODE can be solved to yield:

$$I(s, \mathbf{s}_i) = \int_0^\tau e^{t-\tau} B(t) dt + r_{ij}, \quad [6.3]$$

with  $\tau(s) = \int_0^s \kappa(\zeta) d\zeta$  and  $s$  is the distance along the ray from the boundary. Further,  $r_{ij}$  is given by the boundary condition. With a prescribed temperature on the boundary,  $r_{ij}$  is simply the black boundary intensity at the boundary. In case of reflections  $r_{ij}$  is more complicated. This case is not yet considered.

If  $\kappa$  can be taken constant,  $s$  and  $\tau$  are simply related, and (6.3) can be approximated by a numerical quadrature at point  $i$ :

$$I(\mathbf{x}_j, \mathbf{s}_i) = \sum_{k=1}^{p^{ij}} w_k^{ij} p_k^{ij} = \mathbf{w}^{ij} \cdot \mathbf{p}^{ij} + r_{ij} = \eta_{ij}, \quad [6.4]$$

where we used the notation  $\eta_{ij}$  for the approximation of the intensity at position  $j$  in direction  $i$ . We can rewrite this with (6.2) as:

$$\eta_{ij} = \mathbf{w}^{ij} \cdot \mathbf{T}^{ij} \mathbf{b} + r_{ij} = (\mathbf{T}^{ij})^T \mathbf{w}^{ij} \cdot \mathbf{b} + r_{ij} =: \sum_{k=1}^M a_{ijk} b_k + r_{ij}. \quad [6.5]$$

We see that both the interpolation and the integration have been taken into the tensor  $\mathfrak{A} = (a_{ijk})$ . So, for constant  $\kappa$ , we do not need to store the matrices  $\mathbf{T}^{ij}$  or the vectors  $\mathbf{p}^{ij}$ . If  $\kappa$  is not constant, however, we can write it as a function of the temperature, or  $\kappa = \kappa(B)$ . In (6.4) we should then replace  $\mathbf{w}^{ij}$  with  $\mathbf{w}^{ij}(\mathbf{b})$ . In that case, it is wise to keep at least  $\mathbf{T}^{ij}$  for every  $(i, j)$  in the memory to facilitate the computation of the tensor  $\mathfrak{A}$  according to (6.5). We shall denote the tensor holding the intensity values  $\mathbf{H}$ , so  $\mathbf{H} = (\eta_{ij})$ , and the tensor holding the boundary conditions  $\mathbf{R} = (r_{ij})$ . We then can rewrite (6.5) as:

$$\mathbf{H} = \mathfrak{A} \cdot \mathbf{b} + \mathbf{R}, \quad \text{or} \quad \eta_{ij} = a_{ijk} b_k + r_{ij}, \quad [6.6]$$

using tensor notation and Einstein's summation convention. This equation now allows us to express the intensity at the points in  $\mathfrak{M}$  in terms of the black body intensity, and to eliminate it from the heat equations. Equation (6.6) should be regarded as the more-dimensional variant of the formal solution we used in order to solve the one-dimensional equation.

Now, if we want to express, for example, the incident radiative energy  $G(\mathbf{x})$ , defined by:

$$G(\mathbf{x}) = \int_{4\pi} I(\mathbf{x}, \mathbf{s}) d\Omega,$$

where  $4\pi$  now indicates that we integrate over the whole unit sphere in  $\mathbb{R}^3$  and a unit circle in  $\mathbb{R}^2$ . As in the discussion of the calculation of radiative intensity, we can replace this integral by a quadrature fit for our direction set  $\mathfrak{S}$ , or

$$G(\mathbf{x}) = \sum_{i=1}^N w_i I(\mathbf{x}, \mathbf{s}_i).$$



Evaluated at the points in  $\mathfrak{M}$ , this can be written as

$$\mathbf{g} = (G(\mathbf{x}_1), G(\mathbf{x}_2), \dots, G(\mathbf{x}_M))^T = \mathbf{H}^T \mathbf{w}, \quad \text{or} \quad g_j = \eta_{ij} w_i,$$

in tensor notation, which together with (6.6) leads to

$$g_j = a_{ijk} b_k w_i + r_{ij} w_i.$$

If we now define the matrix  $\mathbf{A} = (\alpha_{ij})$  by  $\alpha_{jk} = w_i a_{ijk}$  and the vector  $\mathbf{f} = (f_j)$  by  $f_j = r_{ij} w_i$ , this is rewritten in the more readable form:

$$\mathbf{g} = \mathbf{A}\mathbf{b} + \mathbf{f}, \quad \text{or} \quad g_j = \alpha_{jk} b_k + f_j. \quad [6.7]$$

If radiation is the only mechanism for heat transfer, the equation describing *steady thermal equilibrium* is

$$\nabla \cdot \mathbf{q}^r(\mathbf{x}) = 4\pi B(\mathbf{x}) - G(\mathbf{x}) = 0.$$

Using (6.1) and (6.7), we can write this as the linear system:

$$4\pi \mathbf{b} = \mathbf{g}, \Leftrightarrow 4\pi \mathbf{b} = \mathbf{A}\mathbf{b} + \mathbf{f}, \Leftrightarrow (4\pi\mathbf{I} - \mathbf{A})\mathbf{b} = \mathbf{f},$$

which we use to solve the heat problem.

## 6.2 Results

We have implemented the described method for simple two dimensional rectangular geometries with black boundaries. Figure 6.1 shows a solution of a pure radiative problem. As we noted before, the number of directions has a larger effect on the error than the number of elements. This is not surprising as the rays initiated by the DOM will always have a large distance between them when far away from the originating point. We also noted a maximum useful number of directions for a given number of elements. Once a good coverage with rays has been reached, additional rays tend to slow the computation process down, rather than deliver more accuracy.

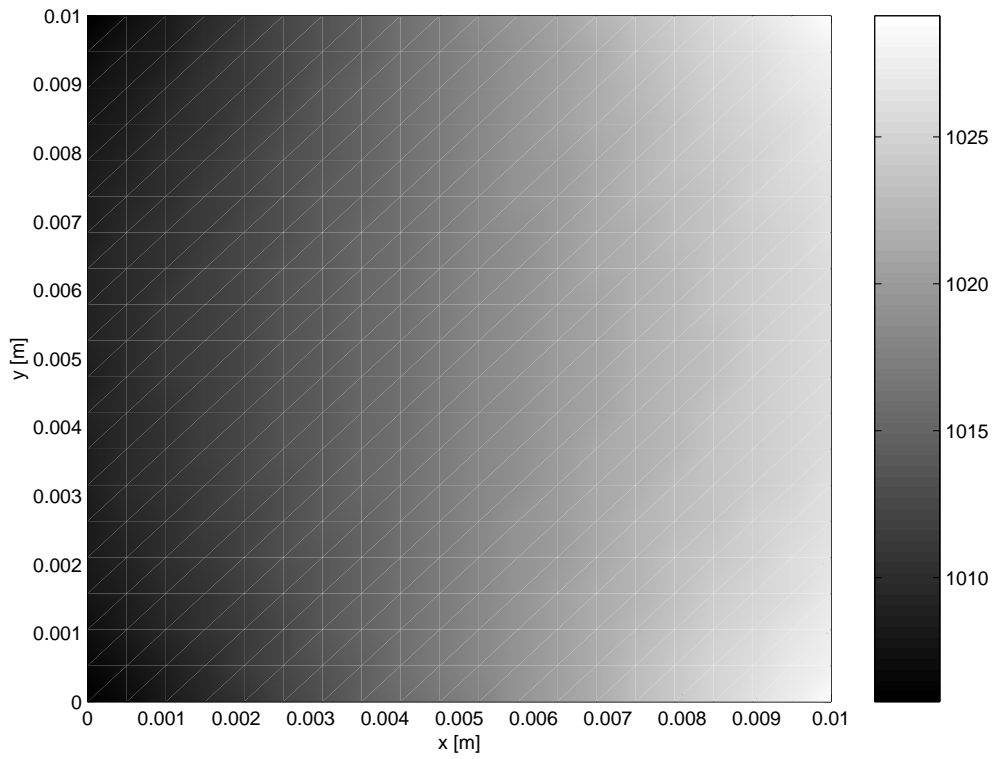


Figure 6.1: Temperature distribution obtained with the algebraic Ray Trace method for a simple pure radiation problem.

## Chapter 7

# Conclusion

Here, we have derived a versatile method for treating radiative heat transfer in semi-transparent materials. Inspired by studies of one-dimensional solution methods, the algebraic form of the Ray Trace Method overcomes the drawbacks of some of the already existing methods: the geometry-unawareness of the Rosseland approximation, the inflexibility for use in forming processes of Fiveland's FEM formulation, and the computational inefficiency of the ray trace method, where we do the costly tracing all over at every time or iteration step.

Because all these methods use the directionally discretised form of the Radiative Transfer Equation, we included a method for finding an optimal set of an arbitrary number of directions with appropriate quadratures. With that approach we can refine the Discrete Ordinate Method arbitrarily.

# Bibliography

- [1] S. Chandrasekhar. *Radiative Transfer*. Dover Publications, Inc., Toronto, 1960.
- [2] W. Fiveland. A finite element method of the discrete ordinate method for multi-dimensional geometries. *Radiative Heat Transfer: Theory and Applications, ASME paper HTD, 244:41–48*, 1993.
- [3] K. Lathrop and B. Carlson. Discrete ordinates angular quadrature of the neutron transport equation. Technical Report 3186, Los Alamos Scientific Laboratory, Los Alamos, N.M., 1964.
- [4] F. Lenters and N. Siedow. Three-dimensional radiative heat transfer in glass cooling processes. Technical Report Berichte Nr. 4, ITWM, Kaiserslautern, 1998.
- [5] D. Mihalas and B. Weibel-Mihalas. *Foundations of Radiation Hydrodynamics*. Oxford University Press, Oxford, 1984.
- [6] M. Modest. *Radiative Heat Transfer*. McGraw-Hill, Inc., Singapore, 1993.
- [7] M. Özişik. *Radiative Transfer and Interactions with Conduction and Convection*. John Wiley and Sons, Inc., Toronto, 1973.